The Responses of Rising or Falling Spherical Wind Sensors to Atmospheric Wind Perturbations

GEORGE H. FICHTL

George C. Marshall Space Flight Center, Ala.

(Manuscript received 20 October 1970, in revised form 26 July 1971)

ABSTRACT

The responses of rising or falling spherical wind sensors to atmospheric wind perturbations are analyzed using Fourier transform techniques. The linearized equations of motion of a sensor that is subject to drag and gravitational body forces are developed by perturbing a sensor about an equilibrium uniform motion with wind fluctuations which have vertical variations. The wind environment and sensor velocities are decomposed with stochastic Fourier-Stieltjes integrals, and the linearized equations of motion are used to derive the response functions and phase angles of the sensor motions. The results of the analysis are used to analyze the response properties of the Jimsphere balloon wind sensor.

The transfer functions and phase angles are functions of the wind perturbation frequency $\omega(=\kappa|\bar{w}|$, κ and $\bar{w}$ being the wavenumber of the perturbation and the mean rise or fall rate of the sensor) and two parameters T and α which are functions of sensor mass, apparent mass of the sensor, the mass of air displaced by the sensor, the mean ascent or descent rate of the sensor as the case may be, and the acceleration of gravity. The quantity T is a time constant of the system and α is the ratio of the apparent mass to the mass of the system. Once these parameters are specified, the response properties of the sensor are completely specified in a linear context. In general, the system becomes more responsive as T and α approach zero and unity, respectively.

As $\omega T \to 0$, the transfer functions and phase angles approach unity and zero, respectively; so that at sufficiently low frequencies, the sensor essentially measures 100% of the wind perturbation Fourier amplitudes with no phase shifts. As $\omega T \to \infty$, the transfer functions and phase angles approach α^2 and zero, respectively; so that at sufficiently large frequencies, the sensor is capable of detecting $100\alpha\%$ of the wind perturbation Fourier amplitudes, again with no phase shifts. If apparent mass effects were not present ($\alpha=0$), the sensor transfer functions would approach zero as $\omega T \to \infty$. Thus, the apparent mass effects make the sensor more responsive. At $\omega T=\alpha^{-\frac{1}{2}}$ for the horizontal fluctuations and $\omega T=2\alpha^{-\frac{1}{2}}$ for the vertical velocity fluctuations, the phase angles of the sensor Fourier amplitudes take on minimum values. In general, the transfer functions associated with the horizontal sensor motions are smaller than the transfer functions associated with the vertical sensor motions in the domain $0<\omega T<\infty$; thus, the sensor is more responsive to vertical than to horizontal air motions.

1. Introduction

The subject of this paper is the responses of rising and falling spherical wind sensors to wind perturbations on the wind profile in the vertical. It has been suggested in various quarters of the meteorological and aerospace communities that it might be possible to detect clear air turbulence and gravity wave phenomena with these devices, which include the Jimsphere spherical balloon (Scoggins, 1967), the ROSE balloon (Brockman, 1964), and the ROBIN falling sphere (Engler, 1965). To determine the capabilities of such devices with respect to measuring small vertical scale wind fluctuations, it is necessary to first determine their response properties. The responses of balloons and falling sphere wind sensors have been the subject of a number of investigations during the last decade (Reed, 1963; Eckstrom, 1965; Leurs and Engler, 1967; Zartarian and Thompson, 1968). However, these investigations have been concerned with the responses of such sensors to vertical variations of the horizontal wind. It now appears that it might be possible to detect vertical velocity fluctuations with these devices, at least with the Jimsphere (DeMandel and Krivo, 1968). Accordingly, the subject of this analysis is the responses of these devices to vertical variations of both the horizontal and vertical components of the wind as they traverse the wind field. The analysis will be based on linear perturbation theory, whereby the wind field is assumed to be composed of a constant basic state mean flow with a superimposed perturbation. Similarly, it is assumed that the associated velocity components of the wind sensor can also be represented in terms of a mean state and a superimposed perturbation. The perturbations are assumed to be sufficiently small, so that nonlinear terms in perturbation quantities can be neglected in comparison to first-order terms. This hypothe-

sis results in a set of three linearized momentum conservation equations that govern the velocity perturbations of the sensor. The subsequent analyses of the response properties of the wind sensors are based on these equations. The Jimsphere is analyzed in detail as an example.

2. Basic equations

The basic equations of motion that govern the behavior of a wind sensor are given by

$$m\frac{du}{dt}=\tfrac{1}{2}\rho C_D A|\mathbf{V}_e-\mathbf{V}|(u_e-u)+m_a\frac{d}{dt}(u_e-u), \quad (1)$$

$$m\frac{dv}{dt}=\tfrac{1}{2}\rho C_D A|\mathbf{V}_e-\mathbf{V}|(v_e-v)+m_a\frac{d}{dt}(v_e-v), \quad (2)$$

$$m\frac{dw}{dt}=\tfrac{1}{2}\rho C_D A|\mathbf{V}_e-\mathbf{V}|(w_e-w)+m_a\frac{d}{dt}(w_e-w)-(m-m_0)g, \quad (3)$$

where m, m_a, A, and C_D denote the mass, apparent mass, cross-sectional area, and drag coefficient of the sensor, respectively; m_0 is the mass of air displaced by the sensor; g the acceleration of gravity; ρ the density of the atmosphere; and t time. The zonal, meridional and vertical components of velocity of the sensor are u, v, and w, respectively; and the subscript e denotes the environmental wind components. The first term on the right side of each equation represents the associated component of the drag force. The drag force is assumed to act parallel and opposite to the direction of the wind vector relative to the sensor, $\mathbf{V}_e-\mathbf{V}$, where

$$\mathbf{V}=u\mathbf{i}+v\mathbf{j}+w\mathbf{k}, \quad (4)$$

$\mathbf{i}$, $\mathbf{j}$ and $\mathbf{k}$ being zonal, meridional, and vertical unit vectors, respectively. The second term on the right side of Eqs. (1)–(3) represents the effects of the sensor apparent mass (Reed, 1963). The third term on the right side of (3) denotes the buoyant force.

The aerodynamic lift forces have been neglected in these equations. The effects of these forces on the sensor motion, in particular the Jimsphere, have been analyzed by Fichtl *et al.* (1971).

3. First-order linear perturbation equations

The environmental wind is assumed to be composed of a constant basic horizontal flow with superimposed velocity fluctuations, so that

$$\left.\begin{aligned} u_e&=\bar{u}_e+u_e'(t)\\ v_e&=\bar{v}_e+v_e'(t)\\ w_e&=w_e'(t)\end{aligned}\right\}, \quad (5)$$

where the overbars and primes denote the basic state and fluctuating parts of the wind. It is assumed that the velocity components of the sensor can also be partitioned into two parts, as was the environmental wind, so that

$$\left.\begin{aligned} u&=\bar{u}+u'(t)\\ v&=\bar{v}+v'(t)\\ w&=\bar{w}+w'(t)\end{aligned}\right\}. \quad (6)$$

The overbarred quantities represent a mean motion of the sensor, and the primed quantities denote the dedepartures from the mean motion. It is now assumed that the basic-state quantities in Eqs. (5) and (6) satisfy Eqs. (1)–(3), and thus it is concluded that

$$\bar{u}=\bar{u}_e, \quad (7)$$

$$\bar{v}=\bar{v}_e, \quad (8)$$

$$\tfrac{1}{2}A\rho C_D|\bar{w}|\bar{w}=(m_0-m)g. \quad (9)$$

These equations govern the mean motion of the sensor. Eqs. (7) and (8) state that the sensor follows the mean horizontal motion of the environment. This results because the horizontal basic-state accelerations of the sensor and the environment vanish. Eq. (9) states that the vertical drag force balances the Archimedean and gravitational body forces. The quantity $\bar{w}$ is the mean ascent or descent rate of the sensor. If $m_0>m$, then $\bar{w}>0$, which corresponds to an ascending sensor; and if $m_0<m$, then $\bar{w}<0$, which corresponds to a descending sensor. An example of the former is the Jimsphere spherical balloon (Scoggins, 1967), while an example of the latter is the ROBIN falling sphere (Engler, 1965).

Substitution of (5) and (6) into Eqs. (1)–(3) and utilization of (7) and (8) yield the equations that govern the perturbations (prime quantities) of the sensor about the unperturbed state; the result is

$$m\frac{du'}{dt}=\tfrac{1}{2}\rho C_D A[(u_e'-u')^2+(v_e'-v')^2+(w_e'-\bar{w}-w')^2]^{\frac{1}{2}}\times(u_e'-u')+m_a\frac{d}{dt}(u_e'-u'), \quad (10)$$

$$m\frac{dv'}{dt}=\tfrac{1}{2}\rho C_D A[(u_e'-u')^2+(v_e'-v')^2+(w_e'-\bar{w}-w')^2]^{\frac{1}{2}}\times(v_e'-v')+m_a\frac{d}{dt}(v_e'-v'), \quad (11)$$

$$m\frac{dw'}{dt}=\tfrac{1}{2}\rho C_D A[(u_e'-u')^2+(v_e'-v')^2+(w_e'-\bar{w}-w')^2]^{\frac{1}{2}}\times(w_e'-\bar{w}-w')+m_a\frac{d}{dt}(w_e'-w')-(m-m_0)g. \quad (12)$$

These equations can be simplified by assuming that the fluctuations of the environmental wind and the sensor components of velocity are infinitesimally small, so that products of perturbation quantities can be neglected in comparison to first-order quantities. Thus,

for infinitesimal perturbations one has

$$m\frac{du'}{dt}=\tfrac{1}{2}\rho C_D A|\bar{w}|(u_e'-u')+m_a\frac{d}{dt}(u_e'-u'), \quad (13)$$

$$m\frac{dv'}{dt}=\tfrac{1}{2}\rho C_D A|\bar{w}|(v_e'-v')+m_a\frac{d}{dt}(v_e'-v'), \quad (14)$$

$$m\frac{dw'}{dt}=\rho C_D A|\bar{w}|(w_e'-w')+m_a\frac{d}{dt}(w_e'-w'), \quad (15)$$

where (9) has been used in deriving (15). These equations state that the fluctuations u', v' and w' are the result of fluctuations in the drag force and the apparent mass terms. The effects resulting from the Archimedean and gravitational body forces are concentrated in the mean motion of the sensor [Eq. (9)].

It should be noted that the environmental velocity fluctuations are being treated as functions of time. Actually the wind field is a function of space and time. As the sensor passes through the wind field, it responds to both the temporal and spatial variations of the wind field. Thus, the sensor yields neither a Lagrangian nor an Eulerian measurement. It shall be assumed that the time scale of the atmospheric motions are sufficiently large compared to the time it takes for the sensor to traverse a particular atmospheric layer, so that the temporal variations of the wind field can be neglected. In addition, it will be assumed that the horizontal variations of the atmospheric wind field are sufficiently large, so that the sensor is essentially responding to vertical variations of the wind field. Thus, in essence, the wind perturbations are assumed to be functions of z only. Now, the explicit time dependence of the wind perturbations indicated in (5) is with respect to the sensor, and is due to the fact that the sensor is ascending through the wind field. To show that this is valid in a linear context, it is noted that the height coordinate z can be transformed to a time coordinate with

$$z=\bar{w}t+\int_0^t w'(\xi)d\xi. \quad (16)$$

Now, $w'(t)$ is a fluctuating quantity, and the negative and positive contributions to the above integral would tend to cancel each other. This means that this integral will fluctuate in sign and, more importantly, will remain small. Now,

$$u_e'(z)=u_e'\left[\left(1+\frac{I'}{\bar{w}t}\right)\bar{w}t\right], \quad (17)$$

where I' denotes the integral in Eq. (16). Upon expanding u_e' in a Maclaurin series about $I'/\bar{w}t=0$, we have

$$u_e'(z)=u_e'(\bar{w}t)+\left(\frac{du_e'}{dz}\right)_{z=\bar{w}t}I'+\cdots. \quad (18)$$

The lead term in this expansion is a linear quantity, and the remaining terms are of second and higher order of smallness; therefore, to be within first order, one has

$$u_e'(z)=u_e'(\bar{w}t), \quad (19)$$

which proves that the environmental wind perturbations can be transformed into explicit functions of time by replacing z with $\bar{w}t$ in the linear problem where $\bar{w}$ is now assumed to be a known quantity. The transformations is not so simple in the nonlinear problem, because the balloon vertical velocity fluctuation w' is contained in the forcing function through the integral I'.

It should be kept in mind that Eqs. (13)–(15) are valid for only sufficiently small perturbation velocity differences ($u_e'-u'$, etc.) compared to the mean rise or fall rate of the sensor. In other words, in order to use (13)–(15) in an analysis of a sensor, we must require that

$$\frac{|u_e'-u'|}{|\bar{w}|},\quad \frac{|v_e'-v'|}{|\bar{w}|},\quad \frac{|w_e'-w'|}{|\bar{w}|}\ll 1. \quad (20)$$

Thus, if we require the magnitudes of the perturbation velocity amplitudes to be less than 0.1 $|\bar{w}|$ in order to satisfy the above inequalities, then the analysis might be acceptable for

$$|u_e'-u'|,\quad |v_e'-v'|,\quad |w_e'-w'|\leqslant 0.1|\bar{w}|. \quad (21)$$

As an example, for the Jimsphere wind sensor (see Section 5) we have $|\bar{w}|\approx 5$ m sec^{-1}, so that the analysis herein will be acceptable for those wind perturbations which have relative velocity magnitudes less than or equal to 0.5 m sec^{-1} according to the above criteria. This may seem to be a severe limitation on the analysis; however, it should be kept in mind that the condition (21) is placed on the perturbation velocity differences rather than individually on the wind and sensor velocity perturbations.

As we shall see later, the major contributions to the relative velocity fluctuation (u_e-u', etc.) come from the short wavelength portion of the wind field with wavelengths <100 m. According to Daniels (1971), the 99th percentile envelope power spectrum along the vertical of detailed zonal wind fluctuations at Cape Kennedy, Fla., is given by

$$\Theta(k)=10.2\times 10^4(4000k)^{-2.43}, \quad (22)$$

where $\Theta(k)$ is the power spectral density [m^2 sec^{-1} (cycle m^{-1})$^{-1}$] at wavenumber k (cycle m^{-1}). This formula was derived from 1200 detailed wind profile measurements in the 5–15 km region with the Jimsphere sensor taken during the years 1965–69. The power spectrum was calculated for each profile for wavenumbers in the interval $0.0005<k<0.01$ cycle m^{-1} and distribution functions of the power spectral estimates were determined for selected wavenumbers in the above stated wavenumber interval. The 99th percentile values

of the power spectral estimates were used to determine the empirical equation (22). If we now assume that (22) can be extrapolated into the region $k>0.01$, then an estimate of the variance of u_e' from wavenumbers in the interval $0.01<k<\infty$ can be obtained by integrating (22) over this interval. This calculation yields a standard deviation of $\sigma=0.3$ m sec^{-1} for the u' perturbations for wavelengths <100 m. If we use σ a typical value of u_e' in an extreme case, then typical values of $|u_e'|/|\bar{w}| \approx 0.06$ in an extreme case for the Jimsphere. As we shall see later, the phase angles δ of the Fourier components of the sensor motion relative to the wind perturbations range between $0<\delta\lesssim 25°$ so that the sensor velocities and environmental velocities will, to a great extent, always tend to be in phase. This means that typically we must have $|u_e'|/|\bar{w}|>|u_e'-u'|/|\bar{w}|$. Thus, in view of above statements concerning $|u_e'|/|\bar{w}|$, it would appear that $|u_e'-u'|/|\bar{w}|\leqslant 0.1$ in most situations for the Jimsphere as required by condition (21). Similar comments hold for the meridional and vertical velocity fluctuations. Accordingly, the linearization of the equations of motion with regard to the velocity fluctuations appears to be valid for the Jimsphere and other spherical wind sensors with comparable rise or fall rates in the troposphere and lower stratosphere.

We close this section with some comments concerning the drag coefficient C_D in (13)–(15). The drag coefficient is defined as

$$C_D=\frac{F_D}{\frac{1}{2}\rho A V_r^2}, \tag{23}$$

where F_D is the magnitude of the drag force and V_r the speed of the air relative to the body. As a sensor ascends or descends through a wind perturbation, the flow relative to the sensor is an accelerating one. This could cause separation of the flow from the sensor and also movement of the separation points so that the aerodynamic drag forces will vary in time. This means the drag coefficient could vary in time, so that fluctuations in the drag force could result from both fluctuations in the relative velocity vector as well as fluctuations in the drag coefficient. Fluctuations in the drag force could result from both fluctuations in the relative velocity vector as well as fluctuations in the drag coefficient. Fluctuations in the drag coefficient might be taken into account by partitioning the drag coefficient into a mean value plus a superimposed fluctuation so that

$$C_D=\bar{C}_D+C_D', \tag{24}$$

where we now treat C_D' as perturbation quantity. Substitution of (5), (6) and (24) into the drag force terms in (1)–(3) and neglecting second- and higher-order products yields the perturbed drag force vector

$$\mathbf{F}_D=-\tfrac{1}{2}\rho A\bar{C}_D|\bar{w}|\bar{w}\mathbf{k}+\tfrac{1}{2}\rho A\bar{C}_D|\bar{w}| \times[(u_e'-u')\mathbf{i}+(v_e'-v')\mathbf{j}+2(w_e'-w)\mathbf{k}] -\tfrac{1}{2}\rho AC_D'|\bar{w}|\bar{w}\mathbf{k}. \tag{25}$$

The first term on the right-hand side of this equation is the steady-state or unperturbed drag force which is balanced by the buoyancy force as stated in (9). The second term in (25) is the contribution to the drag force resulting from perturbations in the environmental wind and sensor velocities. This term corresponds to the perturbation drag forces in Eqs. (13)–(15), and thus the drag coefficient in (13)–(15) can be identified with the steady-state part of the drag coefficient. The third term in (25) is the contribution to the drag force resulting from fluctuations in the drag coefficient and this term only contributes to the vertical component of the drag force. We have not included this term in the vertical perturbation equation (15). Very little is known about the fluctuating part of the drag coefficient in both steady and accelerating flows. The standard practice among aeronautical engineers in problems of this type (response calculations of airplanes, missiles, and projectiles to wind gusts) is to neglect fluctuations in aerodynamic coefficients. We will follow this practice in the analysis that follows. However, we note that the dominant horizontal and vertical velocity fluctuations on the wind profile have vertical wavelengths in the range of 500–1000 m. The time required to traverse these dominant velocity fluctuations for most spherical balloon wind sensors ranges between 100–200 sec. This time is much larger than the time required for the flow around the sensor, and the wake behind the sensor to be established, so that fluctuations in the drag coefficient resulting from acceleration of the flow relative to the sensor would appear to be relatively unimportant. Accordingly, we shall neglect the fluctuating drag coefficient term in the drag force (25). This assumption is the weakest point in the analysis and should be considered as a tentative assumption which should be reviewed as often as drag data on bodies in fluctuating flows become available.

4. Fourier decomposition

Suppose that u_e', v_e' and w_e' are random functions of time, so that u, v and w are also random functions of time. Since random functions are neither periodic nor integrable, neither Fourier series nor integrals may be used in the ordinary sense. Nevertheless, under a set of weak assumptions, a Fourier representation does exist. According to Lumley and Panofsky (1964), the theorem states that the random function $u'(t)$, $v'(t)$ and $w'(t)$ can be expanded in terms of the random function $Z_u(\omega)$, $Z_v(\omega)$ and $Z_w(\omega)$, so that

$$u'(t)=\int_{-\infty}^{\infty} e^{i\omega t}dZ_u(\omega), \tag{26a}$$

with similar integrals for $v'(t)$ and $w'(t)$. Similarly, the environmental wind fluctuation components $u_e'(t)$, $v_e'(t)$ and $w_e'(t)$ can be expanded in terms of the random functions $Z_{u_e}(\omega)$, $Z_{v_e}(\omega)$ and $Z_{w_e}(\omega)$. The Fourier ampli-

tude $dZ_u(\omega)$ is a complex function of ω and is given by

$$dZ_u(\omega)=\lim_{\tau\to\infty}\frac{1}{2\pi}\int_{-\tau}^{\tau}u'(t)e^{-i\omega t}\left(\frac{1-e^{-itd\omega}}{it}\right)dt. \quad (26b)$$

Similar expressions can be written for the remaining random functions.

The equations that govern the Fourier amplitudes of the environmental and sensor velocity fluctuations can be obtained by susbtituting their Fourier integral representations into (13)–(15) and noting that the functions $e^{i\omega t}$ constitute a complete orthogonal function set, so that

$$(1+i\omega T)dZ_u(\omega)=(1+i\alpha\omega T)dZ_{u_e}(\omega), \quad (27)$$

$$(1+i\omega T)dZ_v(\omega)=(1+i\alpha\omega T)dZ_{v_e}(\omega), \quad (28)$$

$$(2+i\omega T)dZ_w(\omega)=(2+i\alpha\omega T)dZ_{w_e}(\omega), \quad (29)$$

where

$$T=\frac{(m+m_a)|\bar{w}|}{|m_0-m|g}, \quad (30)$$

and

$$\alpha=\frac{m_a}{m+m_a}. \quad (31)$$

Division of Eqs. (27) and (28) by $1+i\omega T$ and Eq. (29) by $2+i\omega T$ yields the Fourier amplitudes of the sensor motion, i.e.,

$$dZ_u(\omega)=\frac{1+i\alpha\omega T}{1+i\omega T}dZ_{u_e}(\omega), \quad (32)$$

$$dZ_v(\omega)=\frac{1+i\alpha\omega T}{1+i\omega T}dZ_{v_e}(\omega), \quad (33)$$

$$dZ_W(\omega)=\frac{2+i\alpha\omega T}{2+i\omega T}dZ_{w_e}(\omega). \quad (34)$$

Eqs. (32)–(34) give the Fourier amplitudes of the sensor velocity fluctuations as functions of ω, α, T and the Fourier amplitudes of the environmental wind fluctuations.

5. Transfer functions and phase relationships

The coefficients of $dZ_{u_e}(\omega)$, $dZ_{v_e}(\omega)$ and dZ_{w_e} in (32)–(34) are the system response functions and contain the phase and amplitude information of the sensor velocity fluctuations relative to the environmental wind fluctuations. The amplitude information can be obtained by multiplying each expression by its complex conjugate and then taking an ensemble average. For the zonal fluctuations, one has

$$\langle dZ_u(\omega)dZ_u{}^*(\omega)\rangle=\frac{1+(\alpha\omega T)^2}{1+(\omega T)^2}\langle dZ_{u_e}(\omega)dZ_{u_e}{}^*(\omega)\rangle, \quad (35)$$

where $\langle\ \rangle$ denotes an ensemble average and $(\ )^*$ complex conjugation. The quantity $\langle dZ_u(\omega)dZ_u{}^*(\omega)\rangle$ is the contribution to the variance of u' for frequencies between ω and $\omega+d\omega$, so that

$$\langle dZ_u(\omega)dZ_u{}^*(\omega)\rangle=\phi_u(\omega)d\omega, \quad (36)$$

where $\phi_u(\omega)$ is the spectrum of u'. Similar statements can be made about the remaining random functions. The following relationships between the various spectra follow from Eqs. (32)–(34):

$$\frac{\phi_u(\omega)}{\phi_{u_e}(\omega)}=\frac{\phi_v(\omega)}{\phi_{v_e}(\omega)}=\frac{1+(\alpha\omega T)^2}{1+(\omega T)^2}, \quad (37)$$

$$\frac{\phi_w(\omega)}{\phi_{w_e}(\omega)}=\frac{4+(\alpha\omega T)^2}{4+(\omega T)^2}. \quad (38)$$

The quantities on the right side of these equations are the system transfer functions. As $\omega T\to 0$, the ratios between the sensor velocity spectra and the environmental spectra approach unity, so that the magnitudes of the Fourier amplitudes of the sensor approach the magnitudes of the Fourier amplitudes of the environmental wind fluctuations. As $\omega T\to\infty$, the right-hand sides of (37) and (38) approach α^2. If the apparent mass terms were not present in Eqs. (13)–(15), the system transfer functions would approach zero as $\omega T\to\infty$. Thus, the presence of the derivatives of the environmental wind fluctuations via the apparent mass terms results in the sensor being more responsive to the environment. It should be noted that $\phi_u(\omega)/\phi_{u_e}(\omega)<\phi_w(\omega)/\phi_{w_e}(\omega)$ for $\omega\neq 0$. This means that the sensor filters the horizontal environmental velocity fluctuations more than the vertical environmental velocity fluctuations, or, in other words, the sensor is more responsive to the vertical wind than to the horizontal wind.

The phase angles δ by which the sensor velocity Fourier amplitudes lag behind the environmental Fourier amplitudes can be obtained by calculating the arctangent functions of the ratios of the imaginary and real parts of the system response functions. Thus,

$$\delta_u=\delta_v=\tan^{-1}\left[\frac{(\alpha-1)\omega T}{1+\alpha(\omega T)^2}\right], \quad (39)$$

$$\delta_w=\tan^{-1}\left[\frac{2(\alpha-1)\omega T}{4+\alpha(\omega T)^2}\right]. \quad (40)$$

The phase angles are negative because $\alpha-1<0$. As $\omega T\to 0$ and $\omega T\to\infty$, the arguments of the arctangent functions approach zero, and thus the phase angles approach zero. This means that at both sufficiently small and large frequencies, the sensor and environmental Fourier components are in phase. It follows that the phase angles experience minima at finite values of ωT. Upon differentiating (39) and (40) with respect to

ωT and setting the resulting relationships equal to zero, one finds that δ_u and δ_w experience minima at

$$\left.\begin{aligned}(\omega T)_{\min,u}&=(\omega T)_{\min,v}=\alpha^{-\frac{1}{2}}\\(\omega T)_{\min,W}&=2\alpha^{-\frac{1}{2}}\end{aligned}\right\}. \tag{41}$$

Thus, the minimum phase angle of the horizontal sensor velocity fluctuations occurs at one-half the frequency at which the vertical sensor velocity fluctuations have their minimum phase angle. If the apparent mass effects were not present ($\alpha=0$), the minimum phase angles would all equal 90°, and they would occur at infinitely large frequencies. Substitution of (41) into (39) and (40) will show that minimum phase angles of the horizontal and vertical sensor velocity fluctuations are equal and are given by

$$\delta_{u,\min}=\delta_{v,\min}=\delta_{w,\min}=\tan^{-1}\left(\frac{\alpha-1}{2\alpha^{\frac{1}{2}}}\right). \tag{42}$$

Thus, the minimum phase angles are functions of α only.

6. Jimsphere response

It is instructive to consider a specific example in studies of this nature. In this section the transfer functions and phase angles associated with the Jimsphere wind sensor for standard atmospheric conditions will be calculated. The Jimsphere wind sensor is a spherical, 2m diameter, 0.5-mil, metalized Mylar balloon, fabricated from 12 tailored gores. It has 398 protrusions (cones) approximately 0.08 m high. This sensor is a super-pressurized device with two valves 180° apart to vent helium and thus maintain a superpressure approximately equal to 7 mb. This system has a ballast of 0.1 kg to reduce spurious motions, and the complete system, excluding the inflation gas, has a mass approximately equal to 0.408 kg.

According to Eckstrom (1965), the apparent mass m_a is related to the displaced air m_0 through the relationship

$$m_a=km_0, \tag{43}$$

where k is a dimensionless, experimentally determined parameter. Eckstrom's experimental values for the Jimsphere ranged between 0.46 and 0.58 with an average or characteristic value equal to 0.51.

The total mass of the system is

$$m=m_g+m_s, \tag{44}$$

where m_g and m_s denote the mass of the inflation gas (helium) and the mass of the Jimsphere. The quantity m_s equals 0.408 kg. The mass of the gas m_g can be calculated by assuming that the balloon is in thermal equilibrium with the environment and the excess pressure of the gas within the balloon (approximately 7 mb) with respect to the environment is negligible. Calculations by DeMandel and Krivo (1968) show that departures from thermal equilibrium by as much as 10C and the balloon overpressure produce only a 1.5% variation in the balloon rise rate $\bar{w}$, so that the above assumptions appear reasonable. Thus, utilizing the ideal gas law, one has

$$\frac{m_g}{m_0}=\frac{M_g}{M_0}=\frac{4.0026\text{ gm mole}^{-1}}{28.9644\text{ gm mole}^{-1}}, \tag{45}$$

where M_g and M_0 denote the molecular weights of the sensor gas (helium) and the atmosphere. Since the radius of the Jimsphere is 1 m, the mass of the displaced air is

$$m_0=\tfrac{4}{3}\pi\rho. \tag{46}$$

Substitution of Eqs. (43)–(46) into the expressions for a and T given by (30) and (31) yields

$$T=\frac{k+M_gM_0^{-1}+3m_s(4\pi\rho)^{-1}}{|1-M_gM_0^{-1}-3m_s(4\pi\rho)^{-1}|}\frac{|\bar{w}|}{g}, \tag{47}$$

$$\alpha=\frac{k}{k+M_gM_0^{-1}+3m_s(4\pi\rho)^{-1}}. \tag{48}$$

Fig. 1 gives T and α as functions of altitude calculated with Eqs. (47) and (48). The computations of these curves were based on standard atmosphere values of ρ, the typical rise rates $\bar{w}$ of the Jimsphere balloon as determined by DeMandel and Krivo (1968), and the above mentioned values for the remaining parameters. A typical rise rate of the Jimsphere in the troposphere is 5 m sec^{-1}. It is clear from Fig. 1 that T is approximately equal to 0.5 sec in the first 8 km of the atmosphere. Above the 8-km level T increases rapidly. The quantity α is a monotonically decreasing function of altitude. The quantities α and T are clearly functions of altitude and depend on time through the transformation $z=\bar{w}t$. Thus, in the strictest sense, the perturbation equations (13)–(15) that govern the motion of the sensor are incorrect, because they were derived by assuming constant values for the balloon parameters (C_D, $\bar{w}$, etc.) and atmospheric density, which means that α and T were assumed to be constant. Nevertheless, it appears reasonable, as a first approximation, to apply the transfer functions and phase angle relationships locally at particular altitudes. The assumption here is that α and T do not vary appreciably over thin atmospheric layers with thicknesses that are large compared to the wavelengths of the atmospheric motions of concern. Past studies appear to show that the sensor velocity perturbations with wavelengths $\lesssim$100 m are the ones that depart appreciably from the associated atmospheric perturbations (Zartarian and Thompson, 1968). The departure becomes more pronounced as the wavelength of the atmospheric perturbations becomes small. The quantities α and T have less than 10% vertical variation

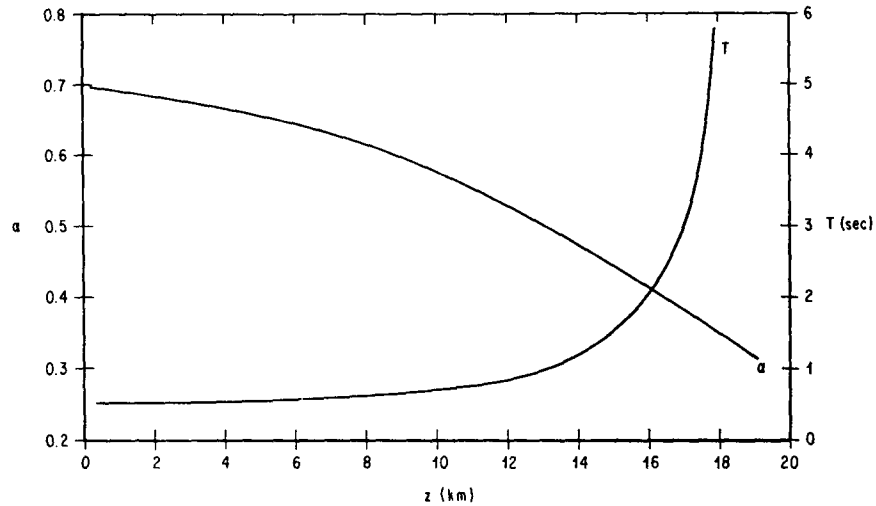

FIG. 1. The quantities T and α as functions of altitude.

over a 1-km thick layer below approximately the 18- and 13-km levels, respectively. Above the 13-km level, T has much larger vertical variation over a 1-km layer. Thus, for example, the quantity T has approximately a 30% vertical variation over a 1-km layer centered at the 17-km level. If 10% variations in α and T over a 1-km layer are accepted to be negligibly small, then it would appear that the analysis in this report could be applied over 1-km thick layers below the 13-km level, because the wavelengths of interest are less than or equal to ~10% of the layer thickness (1 km). Application of the analysis above the 13-km level will only lead to very approximate results. Nevertheless, the theory could be applied to levels above the 13-km level to obtain qualitative results.

Figs. 2–5 are plots of the system transfer functions and the phase angles for $\alpha=0.7$, 0.6, 0.5 and 0.4. For the Jimsphere balloon, these values of α occur at approximately the surface and at the 8.5-, 13- and 16.5-km levels, respectively. The figures show that as α decreases or as height increases, the magnitude of the minimum phase angles increases. The minima occur at $\omega T=\alpha^{-\frac{1}{2}}$ and $2\alpha^{-\frac{1}{2}}$ for the horizontal and vertical wind perturbations, respectively [Eq. (41)]. As α decreases or as height increases, the locations of the minima shift toward larger values of ωT. However T increases faster

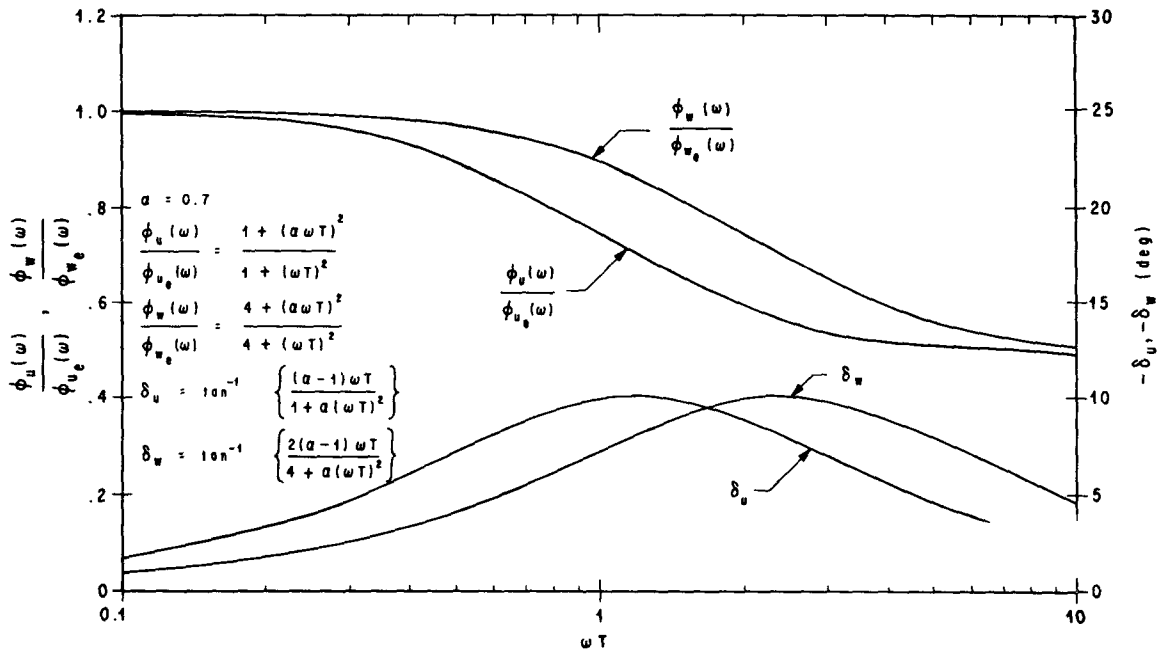

FIG. 2. System transfer functions and phase angles as functions of ωT for $\alpha=0.7$.

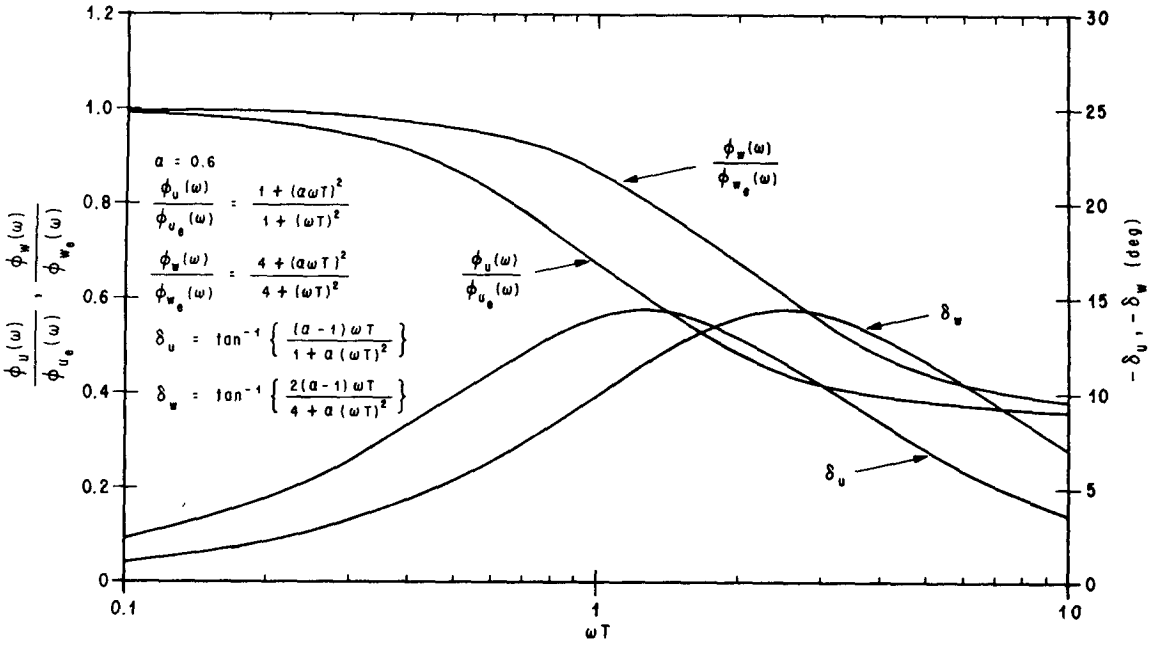

FIG. 3. System transfer functions and phase angles as functions of ωT for $\alpha=0.6$.

than $\alpha^{\frac{1}{2}}$ decreases with height (Fig. 1), and thus the minima actually shift toward smaller values of ω as height increases. This is clearly shown in Fig. 6, a plot of the frequencies $\omega_{\min,u}$, $\omega_{\min,v}$, $\omega_{\min,w}$, at which the minimum phase angles occur as functions of altitude for the horizontal and vertical velocity perturbations of the Jimsphere. The wavelengths at which these minima occur are related to the rise rate through the expression

$$\lambda_{\min}=\frac{2\pi\bar{w}}{\omega_{\min}}. \tag{49}$$

Thus, for example in the troposphere ($z\lesssim 10$ km)$\bar{w}\approx 5$ m sec^{-1}, $\omega_{\min,w}\approx 4.4$ rad sec^{-1}, and $\omega_{\min,u}=\omega_{\min,v}=2.2$ rad sec^{-1}. Substitution of these values into (49)

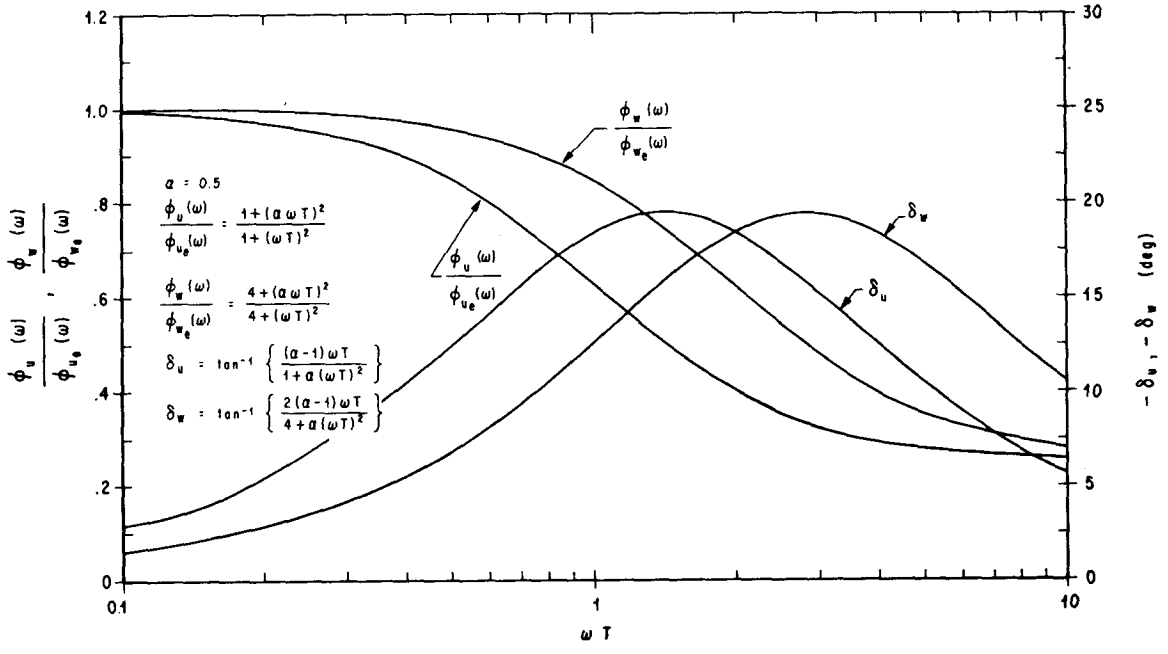

FIG. 4. System transfer functions and phase angles as functions of ωT for $\alpha=0.5$.

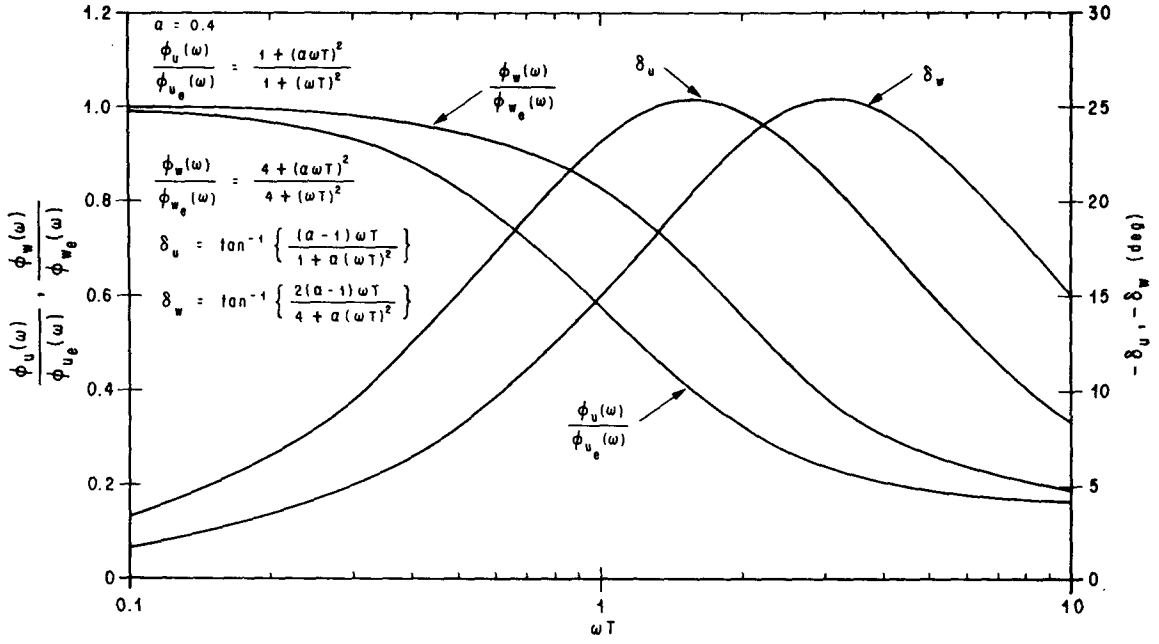

FIG. 5. System transfer functions and phase angles as functions of ωT for $\alpha=0.4$.

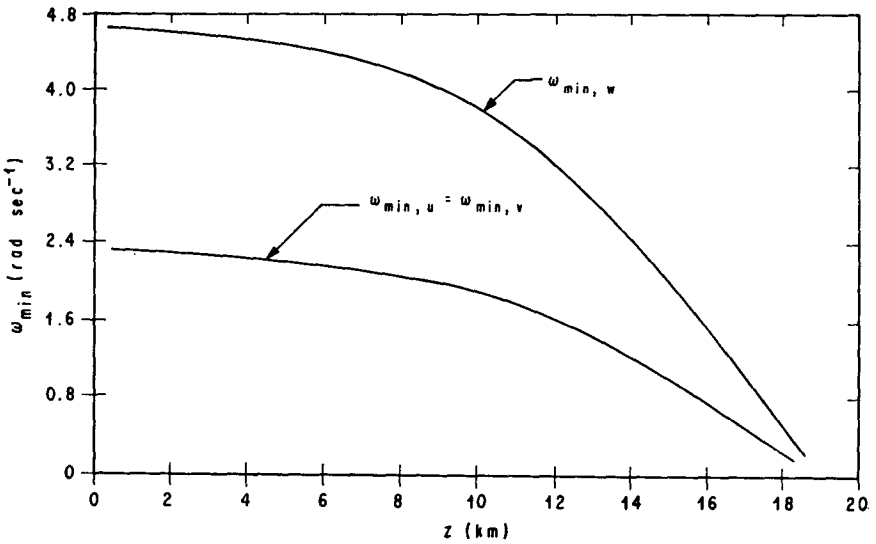

FIG. 6. The frequencies $\omega_{\min,u}$, $\omega_{\min,v}$, and $\omega_{\min,w}$ at which the minimum phase angles occur for the Jimsphere wind sensor as functions of altitude.

yields the corresponding wavelengths $\lambda_{\min,w} \approx 7$ m and $\lambda_{\min,u}=\lambda_{\min,v}\approx 14$ m.

It is clear from Figs. 2–5 that the transfer functions approach α^2 as $\omega T\to\infty$. In fact, the response functions essentially assume constant values at $\omega T=2\pi$, especially for the horizontal velocity fluctuations.

The transfer functions are increasing functions of α and decreasing functions of T. In view of the fact that the quantities α and T are monotonically decreasing and increasing functions of height, respectively, it follows that the transfer functions are decreasing functions of height for any particular value of ω. In short, the Jimsphere becomes less responsive as height increases. An examination of Figs. 2–5 will show that this is indeed the case.

7. Concluding comments

The response of spherical wind sensors to wind perturbations on the wind profile has been analyzed in a linear context. The analysis included aerodynamic drag and buoyancy forces, and apparent mass effects. The

analysis did not include self-induced aerodynamic lift forces.

It is well known that smooth balloon and falling sphere wind sensors execute lateral self-induced motions resulting from aerodynamic lift forces. The nature of these lateral motions is characterized by the Reynolds number

$$\mathrm{Re}=\frac{|\bar{w}|D}{\nu},$$

where D is the diameter of the sensor and ν the coefficient of kinematic viscosity of air. At subcritical Reynolds numbers, for example $\mathrm{Re}\leqslant 2.5\times10^5$, smooth spherical wind sensors execute an orderly spiral motion with the vertical wavelength equal to approximately 12 sensor diameters. These motions constitute a very narrow band process, and for all practical purposes, the spectra of the self-induced motions can be represented with Dirac delta functions. At supercritical Reynolds numbers, $\mathrm{Re}>2.5\times10^5$, the self-induced lateral sensor motions resulting from the unstable wake are erratic in nature and occur over a band of frequencies that is broader than the subcritical one. Scoggins (1967) finds that the addition of approximately 400 conical roughness elements and a point mass of 100 gm to a smooth 2 m diameter balloon essentially eliminates the erratic character of the self-induced sensor motion at supercritical Reynolds numbers, and causes the balloon to execute an orderly narrow band spiral motion or oscillation at both subcritical and supercritical Reynolds numbers with a vertical wavelength of $\sim$24 m. It is clear that the analysis in this report is not valid at those frequencies where aerodynamic lift forces are important. Thus, for example, in the case of the Jimsphere balloon, the analysis herein fails at and in a small neighborhood of frequencies about $\omega=1.3$ rad sec^{-1} ($\lambda=24$ m and $\bar{w}=5$ m sec^{-1}) both for subcritical and supercritical Reynolds numbers. The effects of aerodynamic lift forces on balloon and spherical wind sensors will be considered in a later report.

In the analysis, the effects of radar response in the detection of winds with balloons and falling spheres have also been neglected. DeMandel (1970) finds that radar errors in wind estimates made with the Jimsphere are concentrated in the horizontal and vertical velocity Fourier components with wavelengths smaller than approximately 100 and 200 m, respectively. He also points out that the Fourier components of the radar errors and the wind at these wavelengths are of the same order of magnitude. The effects are indeed important, but are not within the scope of the present report. Nevertheless, the problem of determining the joint response of wind sensors and the tracking radar should be examined in the future.

REFERENCES

Brockman, W. E., 1964: Small scale wind shears from ROSE balloon tracked by AN/FPS-16 Radar. Final Rept., AF 19(604)-7450, University of Dayton, 85 pp.

Daniels, G. E., 1971: Terrestial environment (climatic) criteria guidelines for use in space vehicle development, 1971 revision. TM X-64589, National Aeronautics and Space Administration, 404 pp.

DeMandel, R., 1970: Optimum filters for deriving winds from FPS-16 radar/Jimsphere measurements. *Reprints of Papers Fourth Natl., Conf. Aerospace Meteor.* Las Vegas, Nev., Amer. Meteor. Soc., 136–143.

——, and S. Krivo, 1968: Capability of FPS-16/Jimsphere system for direct measurement of vertical air motions. NASA CR-61232, National Aeronautics and Space Administration, 33 pp.

Eckstrom, C. V., 1965: Theoretical study and engineering development of Jimsphere wind sensor. Final Rept., NAS8-11158, G. T. Schjeldahl Co., 46 pp.

Engler, N. A., 1965: Development of methods to determine winds, density, pressure, and temperature from the ROBIN falling balloon. Final Rept., AF 19(604)-7450, University of Dayton, 141 pp.

Fichtl, G. H., R. E. DeMandel and S. J. Krivo, 1971: Aerodynamic properties of rough spherical balloon wind sensors. NASA TN D-6373, National Aeronautics and Space Administration, 26, pp.

Leurs, J., and N. Engler, 1967: On optimum methods for obtaining wind data from balloon sensors. *J. Appl. Meteor,* 6, 816–823.

Lumley, J., and H. A. Panofsky, 1964: *The Structure of Atmospheric Turbulence.* New York, Interscience, 239 pp.

Reed, W. H., III, 1963: Dynamic response of rising and falling balloon wind sensors with application to estimates of wind loads on launch vehicles. NASA TN D-1821, National Aeronautics and Space Administration, 31 pp.

Scoggins, J. R., 1967: Sphere behavior and the measurement of wind profiles. NASA TN D-3994, National Aeronautics and Space Administration, 53 pp.

Zartarian, G., and J. H. Thompson, 1968: Validity of detailed balloon soundings in booster vehicle design. Sci. Rept. No. 1, AFCRL-68-0606, Kaman Avidyne, 14 pp.